Available online at www.sciencedirect.com
SCIENCE DIRECT®
ELSEVIER
Optics Communications 244 (2005) 389–398
OPTICS COMMUNICATIONS
www.elsevier.com/locate/optcom

Fourier factorization of nonlinear Maxwell equations in periodic media: application to the optical Kerr effect

Nicolas Bonod *, Evgueni Popov, Michel Nevière

Institut Fresnel, case 161, UMR 6133, Université de Provence, Faculté des Sciences et Techniques de St-Jérôme, CLARTE, 13397 Marseille Cedex 20, France

Received 28 May 2004; received in revised form 6 September 2004; accepted 7 September 2004

Abstract

The recently developed fast Fourier factorization method resolves linear Maxwell equations in a truncated Fourier basis using correct factorization rules. In nonlinear optics, Maxwell equations present a discontinuous product of two simultaneously discontinuous functions for which no rule of factorization applies. Using an iterative method which avoids such a type of factorization, we extend the fast Fourier factorization method to nonlinear optics. We demonstrate the good convergence of the method by studying deep metallic gratings with grooves filled with a nonlinear material, illuminated in TM polarization with a high intensity plane wave.

PACS: 42.79.D; 42.65
Keywords: Diffraction gratings optical; Nonlinear optics

1. Introduction

Numerical analysis of periodic media using the differential method requires the projection of Maxwell equations on a truncated basis. It is now well known that the method of factorization of a product of two functions in a truncated Fourier basis [1,2] and more generally on any truncated basis of continuous functions (e.g. Bessel functions [3]), depends on the continuity of the functions and their product. The Laurent's rule gives the Fourier components of a product of two functions in an infinite Fourier basis. As soon as the Fourier basis is truncated, the Laurent's rule, then called "direct rule" presents a bad convergence with respect to the number of Fourier components involved, when the two functions of the product are simultaneously discontinuous. If their product is continuous, it exists another rule, called "inverse rule", which gives

* Corresponding author. Tel.: +33 491288824; fax: +33 491674428.
E-mail address: nicolas.bonod@fresnel.fr (N. Bonod).

0030-4018/$ - see front matter
doi:10.1016/j.optcom.2004.09.026

rapidly converging results. Established in 1996 in a truncated Fourier basis by Li [1] and recently extended in any truncated basis of continuous functions [3], this rule enabled a new formulation of the differential theory of diffraction by periodic media [4]. The new method, called "fast Fourier factorization" (FFF) [2,4] has drastically improved the convergence of the differential method when applied to metallic gratings in TM polarization [4]. However, when the two functions and their product are simultaneously discontinuous, no rule of factorization could enable a good convergence [1], so that the results given by both the direct and the inverse rule have a poor convergence. This is the case in nonlinear optics, when gratings consisting of optically nonlinear materials are considered. In that case, the vector nonlinear polarization can be expressed as the product of a tensor of nonlinear susceptibility by the electric field vector taken at a given power. At the grating surface, the three last functions are simultaneously discontinuous. In that case, the representation of the Fourier components of the product in terms of the two other function Fourier components, using direct or inverse rule is poorly converging. Thus, the factorization of the discontinuous product of discontinuous functions has to be avoided. This paper proposes a method to deal with this problem. The nonlinear problem is treated through an iterative process with respect to the nonlinearity, solving a linear diffraction problem at each iteration step. In the linear diffraction problem, the use of the fast Fourier factorization method allows for the spatial reconstruction of the electric field. The determination of the dielectric permittivity for the next iteration step, is done at any point of the coordinate space from the spatial distribution of the electric field and the nonlinear susceptibility, the latter being zero outside the nonlinear domain and constant inside it. The next iteration resolves a linear diffraction problem with a new spatial distribution of the dielectric permittivity and the fast Fourier transform (FFT) algorithm is then used to find its Fourier components. Such a process, i.e. the calculation of the Fourier components of the dielectric permittivity from its reconstruction in the coordinate space avoids the factorization of a product of type (3) enounced by Li, namely a discontinuous product of two discontinuous functions.

The paper is structured in the following manner. In Section 2, we present the nonlinear Maxwell equations (Section 2.1) from which we deduce the relation between the nonlinear dielectric permittivity and the electric field. Once this relation obtained, we present the iterative method with respect to the nonlinear dielectric permittivity (Section 2.2). We use the FFF method to calculate at each step the Fourier components of the electric field using the direct and the inverse rule (Section 2.3). We have then to calculate for the next iteration the Fourier components of the nonlinear dielectric permittivity.

Once the theoretical method is presented, we show numerical experiments on deep metallic gratings made of nonlinear media illuminated in TM polarization (Section 3.1). Such a configuration requires the use of the FFF method in linear optics. First, we show the convergence of the presented method as a function of the number of Fourier components as it was done in linear optics with the FFF method and the classical differential method (Section 3.2). Then, we study the convergence of the method with respect to the number of iterations (Section 3.3). Then, once the convergence of the method is proved, we study nonlinear effects in metallic gratings illuminated by a plane wave with a high amplitude to obtain large nonlinear effects (Section 3.4).

2. Resolution of nonlinear Maxwell equations using the factorization rules in a truncated Fourier basis

2.1. Maxwell equations in nonlinear optics

Formally, Maxwell equations are the same in linear and nonlinear optic

$$\mathrm{curl}\mathbf{E}(\mathbf{r},t) = -\frac{\partial \mathbf{B}(\mathbf{r},t)}{\partial t}, \tag{1}$$

$$\mathrm{curl}\mathbf{H}(\mathbf{r},t) = \frac{\partial \mathbf{D}(\mathbf{r},t)}{\partial t}, \tag{2}$$

but a nonlinearity will arise from the behaviour of the medium. We consider in this study media without magnetic properties ($\mu(\mathbf{r}) = \mu_0$) and time-independent properties, so that

$$\mathbf{B}(\mathbf{r},t) = \mu_0 \mathbf{H}(\mathbf{r},t), \tag{3}$$

$$\mathbf{D}(\mathbf{r},t) = \varepsilon_0 \mathbf{E}(r,t) + \mathbf{P}(\mathbf{r},t). \tag{4}$$

The particularity of nonlinear optics is the fact that the polarization vector $\mathbf{P}(\mathbf{r},t)$ is split into a linear $\mathbf{P}^{\mathrm{L}}(\mathbf{r},t)$ and a nonlinear $\mathbf{P}^{\mathrm{NL}}(\mathbf{r},t)$ part. In the case of a third-order optical Kerr effect, considering a $\exp(-\mathrm{i}\omega t)$ time dependence and a local response, the nonlinear polarization vector can be written as

$$\begin{aligned}\mathbf{P}^{\mathrm{NL}}(\mathbf{r},t) = \varepsilon_0 \int_{-\infty}^{+\infty} \mathrm{d}\omega_3 \int_{-\infty}^{+\infty} \mathrm{d}\omega_2 \\ \int_{-\infty}^{+\infty} \chi^{\mathrm{ker}\,r}_{\omega_1,\omega_2,\omega_3}(\mathbf{r}) \mathbf{E}_{\omega_1}(\mathbf{r}) \mathbf{E}_{\omega_2}(\mathbf{r}) \mathbf{E}_{\omega_3}(\mathbf{r}) \\ \times \exp(-\mathrm{i}(\omega_1+\omega_2+\omega_3)t)\mathrm{d}\omega_1,\end{aligned} \tag{5}$$

where $\chi^{\mathrm{ker}\,r}_{\omega_1,\omega_2,\omega_3}$ is a fourth-rank tensor, and $\mathbf{E}_{\omega,j}(\mathbf{r}) = \frac{1}{2\pi}\int_{-\infty}^{+\infty} \mathbf{E}(\mathbf{r},t)\exp(\mathrm{i}\omega_j t)\,\mathrm{d}t, \quad j = 1:3.$ In the same way, we define

$$\mathbf{P}_\omega(\mathbf{r}) = \frac{1}{2\pi}\int_{-\infty}^{+\infty} \mathbf{P}(\mathbf{r},t)\exp(\mathrm{i}\omega t)\,\mathrm{d}t. \tag{6}$$

The optical Kerr effect is a third-order effect which assumes: $\omega_1 = \omega_3 = -\omega_2$, which leads to

$$\mathbf{P}^{\mathrm{NL}}_\omega(\mathbf{r}) = \varepsilon_0 \chi^{\mathrm{Kerr}}_\omega \mathbf{E}_\omega(\mathbf{r}) \overline{\mathbf{E}}_\omega(\mathbf{r}) \mathbf{E}_\omega(\mathbf{r}), \tag{7}$$

with the notation $\chi^{\mathrm{Kerr}}_\omega = \chi^{\mathrm{ker}\,r}_{\omega,\omega,\omega}$ and where $\overline{\mathbf{E}}_\omega(\mathbf{r})$ is the complex conjugate of $\mathbf{E}_\omega(\mathbf{r})$. In Kerr media, $\mathbf{D}_\omega(\mathbf{r})$ is written as

$$\begin{aligned}\mathbf{D}_\omega(\mathbf{r}) &= \varepsilon_0 \mathbf{E}_\omega(\mathbf{r}) + \mathbf{P}_\omega(\mathbf{r}) \\ &= \varepsilon_0 \mathbf{E}_\omega(\mathbf{r}) + \mathbf{P}^{\mathrm{L}}_\omega(\mathbf{r}) + \mathbf{P}^{\mathrm{NL}}_\omega(\mathbf{r}) \\ &= \varepsilon_0 \mathbf{E}_\omega(\mathbf{r}) + \varepsilon_0 \chi^1_\omega(\mathbf{r}) \mathbf{E}_\omega(\mathbf{r}) \\ &\quad + \varepsilon_0 \chi^{\mathrm{Kerr}}_\omega(\mathbf{r}) \mathbf{E}_\omega(\mathbf{r}) \overline{\mathbf{E}}_\omega(\mathbf{r}) \mathbf{E}_\omega(\mathbf{r}),\end{aligned} \tag{8}$$

$$\mathbf{D}_\omega(\mathbf{r}) = \varepsilon_0(1 + \chi^1_\omega(\mathbf{r}) + \varepsilon_0 \chi^{\mathrm{Kerr}}_\omega(\mathbf{r}) E_\omega(\mathbf{r}) \overline{\mathbf{E}}_\omega(\mathbf{r})) \mathbf{E}_\omega(\mathbf{r}). \tag{9}$$

Finally, we can write

$$\mathbf{D}_\omega(\mathbf{r}) = \varepsilon_\omega(\mathbf{r}) \mathbf{E}_\omega(\mathbf{r}), \tag{10}$$

and the dielectric tensor $\varepsilon(\mathbf{r})$ is split into a linear part $\varepsilon^{\mathrm{L}}(\mathbf{r})$ and a nonlinear part $\varepsilon^{\mathrm{NL}}(\mathbf{r})$

$$D_\omega(r) = \varepsilon^{\mathrm{L}}_\omega E(r) + \varepsilon^{\mathrm{NL}}_\omega E(r), \tag{11}$$

with

$$\varepsilon^{\mathrm{L}}_\omega(\mathbf{r}) = \varepsilon_0(1 + \chi^1_\omega(\mathbf{r})), \tag{12}$$

and

$$\varepsilon^{\mathrm{NL}}_\omega(\mathbf{r}) = \varepsilon_0 \chi^{\mathrm{Kerr}}_\omega(\mathbf{r}) \boldsymbol{E}_\omega(\mathbf{r}) \overline{\boldsymbol{E}}_\omega(\mathbf{r}). \tag{13}$$

If the dielectric permittivity were known in Eq. (10), it would be possible to rigorously resolve Maxwell equations using the factorization rules. This is done through an iterative method which calculates at each step the electric field, from which we deduce the dielectric permittivity from Eq. (13).

2.2. Iterative method

One way to rigorously resolve the nonlinear Maxwell equations is to make iterations with respect to the nonlinear permittivity, resolving a linear diffraction problem at each step. The first iteration corresponds to the linear case. The nonlinear effect lies in the change of the dielectric permittivity tensor $\varepsilon(r)$. The second iteration is made replacing the linear dielectric permittivity of the grating media with the new one calculated with Eq. (13) where the electric field is the one calculated during the preceding iteration step.

Due to the periodicity of the device, we project Maxwell equations onto a pseudo-Fourier basis. In view of solving numerically the equations, we must truncate the basis to $2N + 1$ unknown Fourier components of the electric and magnetic field. These components are put into columns vectors denoted [**E**] and [**H**]. Eq. (13) contains product of functions so that a factorization must be made, using suitable factorization rules. It will be done in the same way as the one used in the FFF method, the difference lying in the fact that iterations have to be considered. In view of linearizing Maxwell equations (Eqs. (1) and (2)), we rewrite Eq. (10), at the $\{j\}$th iteration step, as

$$\mathbf{D}^{\{j\}}_{\omega,\mathrm{NL}} = \varepsilon^{\{j-1\}}_{\omega,\mathrm{NL}} E^{\{j\}}_{\omega,\mathrm{NL}}, \tag{14}$$

so that the new set of linearized Maxwell equations reads

$$\mathrm{curl}\mathbf{E}^{\{j\}}_{\omega,\mathrm{NL}} = \mathrm{i}\omega\mu_0 \mathbf{H}^{\{j\}}_{\omega,\mathrm{NL}}, \tag{15}$$

$$\mathrm{curl}\mathbf{H}^{\{j\}}_{\omega,\mathrm{NL}} = -\mathrm{i}\omega\varepsilon^{\{j-1\}}_{\omega,\mathrm{NL}}\mathbf{E}^{\{j\}}_{\omega,\mathrm{NL}}. \quad (16)$$

In Eq. (14), the product $\varepsilon^{\{j-1\}}_{\omega,\mathrm{NL}}\mathbf{E}^{\{j\}}_{\omega,\mathrm{NL}} = \mathbf{D}^{\{j\}}_{\omega,\mathrm{NL}}$ is a discontinuous product of discontinuous functions. To do its factorization, we introduce a continuous vector $\mathbf{F}^{\{j\}}_{\varepsilon,\omega,\mathrm{NL}}$ defined by

$$\mathbf{F}^{\{j\}}_{\varepsilon,\omega,\mathrm{NL}} = \begin{pmatrix} E^{\{j\}}_{\omega,\mathrm{NL},\mathbf{T}_1} \\ D^{\{j\}}_{\omega,\mathrm{NL},\mathbf{N}} \\ E^{\{j\}}_{\omega,\mathrm{NL},\mathbf{T}_2} \end{pmatrix}, \quad (17)$$

where $\mathbf{T}_1$, $\mathbf{T}_2$ are two tangential vectors to the grating surface, $\mathbf{N}$ is its normal vector, and $\mathbf{E}^{\{j\}}_{\omega,\mathrm{NL},\mathbf{T}_1} = \mathbf{E}^{\{j\}}_{\omega,\mathrm{NL}} \cdot \mathbf{T}_1$. This continuous vector $\mathbf{F}^{\{j\}}_{\varepsilon,\omega,\mathrm{NL}}$ is related to the discontinuous electric field vector by the relation

$$\mathbf{E}^{\{j\}}_{\omega,\mathrm{NL}} = C^{\{j-1\}}_{\varepsilon,\omega,\mathrm{NL}}\mathbf{F}^{\{j\}}_{\varepsilon,\omega,\mathrm{NL}}, \quad (18)$$

where $C^{\{j-1\}}_{\varepsilon,\omega,\mathrm{NL}}$ is a $3(2N+1) \times 3(2N+1)$ matrix, so that Eq. (14) becomes

$$\mathbf{D}^{\{j\}}_{\omega,\mathrm{NL}} = \varepsilon^{\{j-1\}}_{\omega,\mathrm{NL}}C^{\{j-1\}}_{\varepsilon,\omega,\mathrm{NL}}\mathbf{F}^{\{j\}}_{\varepsilon,\omega,\mathrm{NL}}. \quad (19)$$

$\mathbf{F}^{\{j\}}_{\varepsilon,\mathrm{NL}}$ being continuous, the factorization is done using the direct rule

$$\left[\mathbf{D}^{\{j\}}_{\omega,\mathrm{NL}}\right] = [\![\varepsilon^{\{j-1\}}_{\omega,\mathrm{NL}}C^{\{j-1\}}_{\varepsilon,\omega,\mathrm{NL}}]\!]\left[\mathbf{F}^{\{j\}}_{\varepsilon,\omega,\mathrm{NL}}\right], \quad (20)$$

where $[\![f]\!]$ is the Toeplitz matrix whose (n,m) entry is f_{n-m}. In a second step, we have to do the factorization of the continuous product

$$\mathbf{F}^{\{j\}}_{\varepsilon,\omega,\mathrm{NL}} = \left(C^{\{j-1\}}_{\varepsilon,\omega}\right)^{-1}\mathbf{E}^{\{j\}}_{\omega,\mathrm{NL}}. \quad (21)$$

This is done using the inverse rule

$$\left[\mathbf{F}^{\{j\}}_{\varepsilon,\omega,\mathrm{NL}}\right] = [\![C^{\{j-1\}}_{\varepsilon,\omega,\mathrm{NL}}]\!]^{-1}\left[\mathbf{E}^{\{j\}}_{\omega,\mathrm{NL}}\right]. \quad (22)$$

We thus obtain

$$\begin{aligned}\left[\mathbf{D}^{\{j\}}_{\omega,\mathrm{NL}}\right] &= [\![\varepsilon^{\{j-1\}}_{\omega,\mathrm{NL}}C^{\{j-1\}}_{\varepsilon,\omega,\mathrm{NL}}]\!]\left[\mathbf{F}^{\{j\}}_{\omega,\mathrm{NL}}\right] \\ &= [\![\varepsilon^{\{j-1\}}_{\omega,\mathrm{NL}}C^{\{j-1\}}_{\varepsilon,\omega,\mathrm{NL}}]\!][\![C^{\{j-1\}}_{\varepsilon,\omega,\mathrm{NL}}]\!]^{-1}\left[\mathbf{E}^{\{j\}}_{\omega,\mathrm{NL}}\right]. \quad (23)\end{aligned}$$

Introducing a matrix $Q^{\{j-1\}}_{\varepsilon,\omega,\mathrm{NL}}$ defined by

$$Q^{\{j-1\}}_{\varepsilon,\omega,\mathrm{NL}} = [\![\varepsilon^{\{j-1\}}_{\omega,\mathrm{NL}}C^{\{j-1\}}_{\varepsilon,\omega,\mathrm{NL}}]\!][\![C^{\{j-1\}}_{\varepsilon,\omega,\mathrm{NL}}]\!]^{-1}, \quad (24)$$

the factorization of the product in Eq. (14) finally reads

$$\left[\mathbf{D}^{\{j\}}_{\omega,\mathrm{NL}}\right] = Q^{\{j-1\}}_{\varepsilon,\omega,\mathrm{NL}}\left[\mathbf{E}^{\{j\}}_{\omega,\mathrm{NL}}\right]. \quad (25)$$

This shows that the Toeplitz matrix $[\![\varepsilon^{\{j-1\}}_{\omega,\mathrm{NL}}]\!]$ which would have been introduced by the Laurent's rule applied to Eq. (14) has indeed to be replaced by the more complicated matrix $Q^{\{j-1\}}_{\varepsilon,\omega,\mathrm{NL}}$. It is then possible, as was done in the FFF method [2–4], to express the M matrix defined by

$$\frac{\mathrm{d}}{\mathrm{d}y}\begin{pmatrix}\left[E^{\{j\}}_{x,\omega,\mathrm{NL}}\right] \\ \left[E^{\{j\}}_{z,\omega,\mathrm{NL}}\right] \\ \left[H^{\{j\}}_{x,\omega,\mathrm{NL}}\right] \\ \left[H^{\{j\}}_{z,\omega,\mathrm{NL}}\right]\end{pmatrix} = \mathbf{M}^{\{j-1\}}_{\omega,\mathrm{NL}}\begin{pmatrix}\left[E^{\{j\}}_{x,\omega,\mathrm{NL}}\right] \\ \left[E^{\{j\}}_{z,\omega,\mathrm{NL}}\right] \\ \left[H^{\{j\}}_{x,\omega,\mathrm{NL}}\right] \\ \left[H^{\{j\}}_{z,\omega,\mathrm{NL}}\right]\end{pmatrix}. \quad (26)$$

Solving the nonlinear Maxwell equations requires the calculation of the matrix $\mathbf{M}^{\{j-1\}}_{\omega,\mathrm{NL}}$ with the values of the nonlinear dielectric permittivity calculated at the end of the preceding iteration. We thus need to calculate the Fourier components of the nonlinear dielectric permittivity defined by Eqs. (12) and (13). Let us examine the continuity of the different functions in view of making the factorization of Eq. (13). The term $\varepsilon^{\mathrm{NL}}_{\omega}(\mathbf{r})$ vanishes outside the nonlinear medium, so that the product in Eq. (13) is always discontinuous across the boundary of a nonlinear medium. If the electric field components are discontinuous, this product corresponds to the case 3 enounced by Li [1] for which no factorization rule can be applied. Nevertheless, it is possible to calculate its Fourier components using the FFT algorithm if the dependence of $\varepsilon^{\{j-1\}}_{\mathrm{NL}}(\mathbf{r})$ with respect to $\mathbf{r}$ is known. This can be made using Eq. (13), but it requires the knowledge of the electric field map in the coordinate space.

2.3. Electric field map reconstruction and calculation of the Fourier components of the dielectric permittivity

At the end of the $\{j-1\}$th iteration, in view of calculating the electromagnetic field map, we lay out the Fourier components $[E^{\{j-1\}}_{x,\omega,\mathrm{NL}}]$, $[E^{\{j-1\}}_{z,\omega,\mathrm{NL}}]$, $[H^{\{j-1\}}_{x,\omega,\mathrm{NL}}]$, and $[H^{\{j-1\}}_{z,\omega,\mathrm{NL}}]$. We deduce at an any ordinate y_i the Fourier components $[E^{\{j-1\}}_{y,\omega,\mathrm{NL}}]$ from Maxwell equations which result in

$$\left[E^{\{j\}}_{y,\omega,\mathrm{NL}}\right] = -\left(Q^{\{j-1\}}_{\varepsilon,yy}\right)^{-1}\left\{\omega_{\mathrm{NL}}^{-1}\left(\gamma_0\left[H^{\{j\}}_{x,\omega,\mathrm{NL}}\right] - \alpha_{\mathrm{NL}}\left[H^{\{j\}}_{z,\omega,\mathrm{NL}}\right]\right) + Q^{\{j-1\}}_{\varepsilon,yx}\left[E^{\{j\}}_{x,\omega,\mathrm{NL}}\right] + Q^{\{j-1\}}_{\varepsilon,yz}\left[E^{\{j\}}_{z,\omega,\mathrm{NL}}\right]\right\}. \quad (27)$$

But, because of the discontinuities of $\mathbf{E}^{j-1}_{\omega,\mathrm{NL}}(\mathbf{r})$, its reconstruction from its Fourier components will lead to Gibbs phenomenon. We thus have to reconstruct a continuous vector, namely $\mathbf{F}^{(j-1)}_{\varepsilon,\omega,\mathrm{NL}}$ defined by Eq. (22). Once the components $[E^{\{j-1\}}_{x,y,z,\omega,\mathrm{NL}}]$ are known, one can calculate the Fourier components of the field vector $[\mathbf{F}^{\{j-1\}}_{\varepsilon,\omega,\mathrm{NL}}]$ using Eq. (22): $[\mathbf{F}^{\{j-1\}}_{\varepsilon,\omega,\mathrm{NL}}] = [\![C^{\{j-2\}}_{\varepsilon,\omega}]\!]^{-1}[\mathbf{E}^{\{j-1\}}_{\omega,\mathrm{NL}}]$. The summation of the truncated Fourier series

$$\mathbf{F}^{\{j-1\}}_{\varepsilon,\omega,\mathrm{NL}}(\mathbf{r}) = \sum_{m=-N}^{N}\left[\mathbf{F}^{\{j-1\}}_{\varepsilon,\omega,\mathrm{NL}}\right]_{mn} \times \exp[\mathrm{i}\alpha_{\mathrm{NL},m}x + \mathrm{i}\gamma_0 z], \quad \forall\ y_i, \quad (28)$$

in view of obtaining $\mathbf{F}^{\{j-1\}}_{\varepsilon,\omega,\mathrm{NL}}(\mathbf{r})$ does not introduce any Gibbs phenomenon, because $\mathbf{F}^{\{j-1\}}_{\varepsilon,\omega,\mathrm{NL}}(\mathbf{r})$ is a continuous function of the spatial coordinates. Using the matrix $C^{\{j-2\}}_{\varepsilon,\omega}(\mathbf{r})$ enables us to calculate $\mathbf{E}^{\{j-1\}}_{\omega,\mathrm{NL}}(\mathbf{r})$

$$\mathbf{E}^{\{j-1\}}_{\omega,\mathrm{NL}}(\mathbf{r}) = C^{\{j-2\}}_{\varepsilon,\omega,\mathrm{NL}}(\mathbf{r})\mathbf{F}^{\{j-1\}}_{\varepsilon,\omega,\mathrm{NL}}(\mathbf{r}). \quad (29)$$

We thus obtain the nonlinear part of the dielectric tensor

$$\varepsilon^{\mathrm{Kerr}\{j-1\}}_{\omega}(\mathbf{r}) = \varepsilon_0\chi_{\omega}(\mathbf{r})\mathbf{E}^{\{j-1\}}_{\omega,\mathrm{NL}}(\mathbf{r})\overline{\mathbf{E}}^{\{j-1\}}_{\omega,\mathrm{NL}}(\mathbf{r}). \quad (30)$$

The programming is then the same as in the linear case. It just requires to store the matrices $Q^{\{j-1\}}_{\varepsilon,\omega,\mathrm{NL}}$ in order to calculate matrix $M^{\{j-1\}}_{\varepsilon,\omega,\mathrm{NL}}$, to store $[\![C^{\{j-1\}}_{\varepsilon,\omega,\mathrm{NL}}]\!]$ to calculate $[\mathbf{F}^{\{j\}}_{\varepsilon,\omega,\mathrm{NL}}]$, and to store $C^{\{j-1\}}_{\varepsilon,\omega,\mathrm{NL}}(\mathbf{r})$ to calculate $\mathbf{E}^{\{j\}}_{\omega,\mathrm{NL}}(\mathbf{r})$ and $\varepsilon^{\{j\}}_{\mathrm{NL}}(\mathbf{r})$. When M is y dependent, a numerical integration is necessary to resolve Eq. (26). In a lamellar grating, the M matrix is y independent in the first iteration but due to the nonlinearity, from the second iteration, the map of the dielectric permittivity is y dependent, and as a consequence, the M matrix is y dependent and a numerical integration process is also necessary.

The next numerical study lying on metallic gratings where the nonlinear medium is inside the grooves, a large groove depth will be considered in order to obtain a significant nonlinear effect. As a consequence, numerical problems will arise when integrating Eq. (26). That is the reason why we use the S-matrix propagation algorithm [4,5] which avoids numerical problems when integrating in deep metallic gratings.

3. Convergence of the method

3.1. Optogeometrical parameters of the numerical study

The device under study is chosen in such a way that, in the linear case, the classical differential method will not be convergent. That is the reason why we choose a metallic grating illuminated in TM polarization. Moreover, we want the factorization of the product $\varepsilon^{\mathrm{Kerr}\{j-1\}}_{\omega}(\mathbf{r}) = \varepsilon_0\chi^{\mathrm{Kerr}}_{\omega}(\mathbf{r})\mathbf{E}^{\{j-1\}}_{\omega}(\mathbf{r})\overline{\mathbf{E}}^{\{j-1\}}_{\omega}(\mathbf{r})$ to be not convergent using inverse or direct rule, i.e. when the electric field and the nonlinear susceptibility are simultaneously discontinuous. This is the case when the nonlinear media is inside the groove.

In order to obtain a significant nonlinear effect, we have to choose deep grooves, and the optogeometrical parameters are chosen to obtain a resonance inside the groove. A cavity resonance may lead to a significant increase of the electric field inside the groove, which contains the nonlinear media. We consider in a first time a lamellar metallic grating as illustrated in Fig. 1. It is illuminated

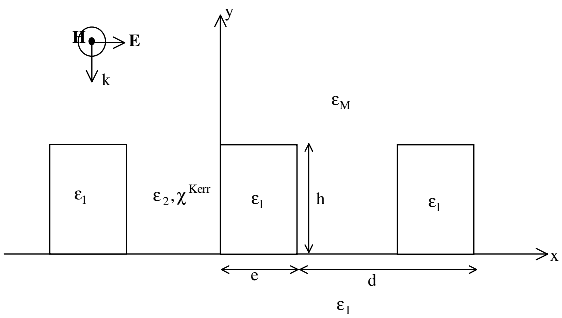

Fig. 1. Schematic representation of the grating. The substrate and the pillars are denoted 1 with a relative permittivity $\varepsilon_{r1} = -182.4 + i43.52$ the superstrate is denoted M with $\varepsilon_{rM} = 1$ and the grooves are denoted 2, with $\varepsilon_{r2} = 12.04$ nm. $\chi = 10^{-6}$ esu, $h =$ 494 nm, $d = 2e$ =1000 nm.

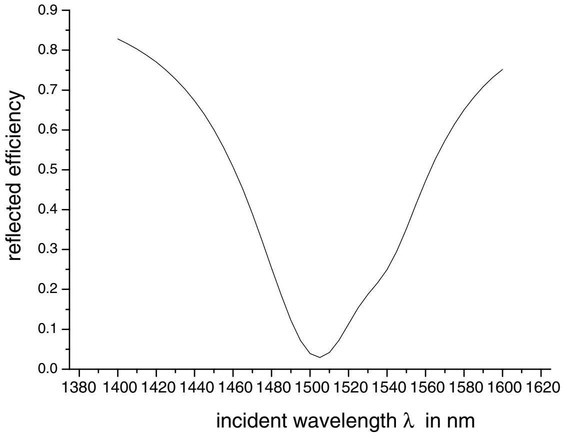

Fig. 2. Reflected efficiency as a function of the incident wavelength with the optogeometrical parameters of Fig. 1. Presence of a resonance at a wavelength around 1500 nm.

in normal incidence and in TM polarization. The incident wavelength is $\lambda = 1500$ nm. The substrate is made of the same metal as in the pillars, and the superstrate is air. With such parameters, the zeroth reflected order is the only propagative one. The amplitude of the incident field is equal to 10^6 V/m in order to increase the nonlinear effects. The nonlinear dielectric medium chosen is silicon and is isotropic, so that [6]

$$[\chi_{\omega}^{\mathrm{Kerr}}]_{i,j,k,l} = \chi(\delta_{i,j}\delta_{k,l} + \delta_{i,k}\delta_{j,l} + \delta_{i,l}\delta_{j,k}). \qquad (31)$$

Different unity systems exist, so following our notations, we express χ in the SI system [6]:

$$(\chi)_{\mathrm{SI}} = (\chi)_{\mathrm{esu}} \frac{4\pi}{(3\times 10^4)^2} \equiv [\mathrm{V}^{-2}\ \mathrm{m}^2]. \qquad (32)$$

In view of testing the good convergence of the theory when strong nonlinear effects occur, we choose $\chi = 10^{-6}$ esu in silicon, which is 2 orders of magnitude larger than the one used in [7]. The groove depth is chosen equal to $h = 494$ nm, a value for which we obtain a resonance process. Fig. 2 represents the reflected efficiency as a function of the wavelength. For a wavelength close to 1500 nm, we obtain a minimum of the reflectivity. This almost total absorption of the light by the grating

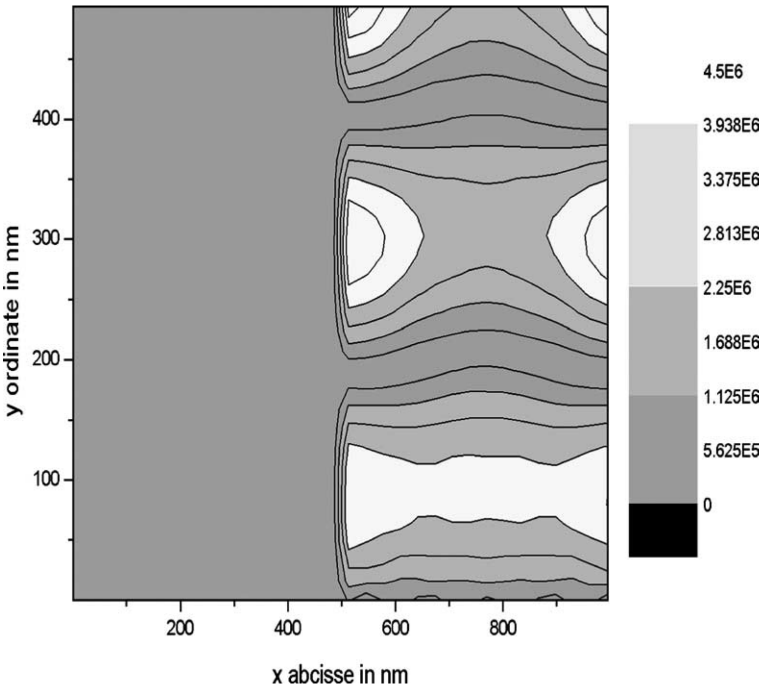

Fig. 3. |**E**| electric field reconstruction in the grating with $\lambda = 1500$ nm using the correct reconstruction method avoiding Gibbs phenomenon; $N = 22$.

is linked with the local field enhancement which occurs at resonance.

3.2. Field map reconstruction and Gibbs phenomenon

To determinate the type of resonance occurring around $\lambda = 1500$ nm, we have to visualize the electric field inside the grating when the reflectivity is minimized. We only consider the first iteration step, which corresponds to the linear case. We apply the fast Fourier factorization method to calculate at each ordinate inside the modulated region the Fourier components of the electric field. To obtain the electric field map reconstruction, as explained in Section 2.3, we can calculate the electric field in the space coordinates directly from its Fourier components, which may lead to Gibbs oscillations, or from the reconstruction of the continuous vector $\mathbf{F}_{\varepsilon,\omega,\mathrm{NL}}$, using Eqs. (29) and (30). We plot in Fig. 3, the electric field-map reconstruction inside a grating groove without Gibbs phe-

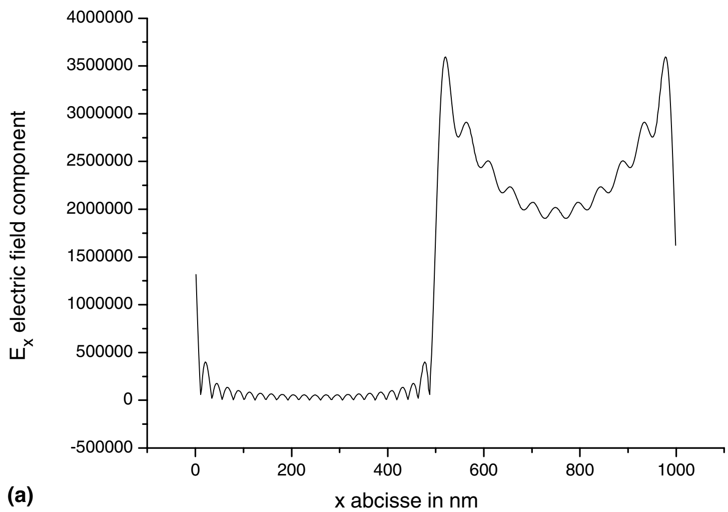

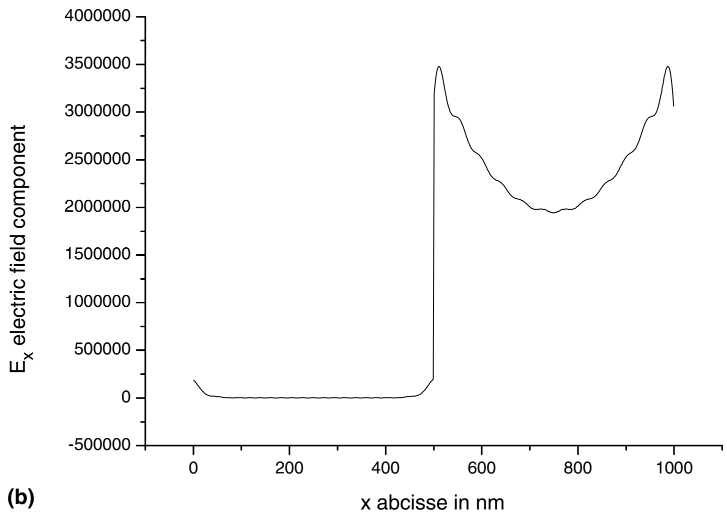

Fig. 4. Reconstruction of the $|E_x|$ electric field component as a function of the x variable calculated at ordinate $y_i = 300$ nm: (a) with Gibbs phenomenon, (b) without Gibbs phenomenon. Number of Fourier components: $N = 22$; $\lambda = 1500$ nm.

nomenon. As it was expected, we can observe in the nonlinear media the presence of three areas where the electric field amplitude is high. In these areas the nonlinear effects will be the strongest. We denote "cavity resonance" this type of resonance.

In order to visualize the difference between the two field reconstruction methods, we plot in Fig. 4 the discontinuous E_x electric field component calculated at an ordinate y_i ($y_i = 300$ nm) as a function of the x variable. In Fig. 4(a), when the field is reconstructed directly from its Fourier components, we can observe the presence of oscillations, which is a characteristic of the Gibbs phenomenon. In Fig. 4(b), the electric field is derived from the reconstruction of the continuous

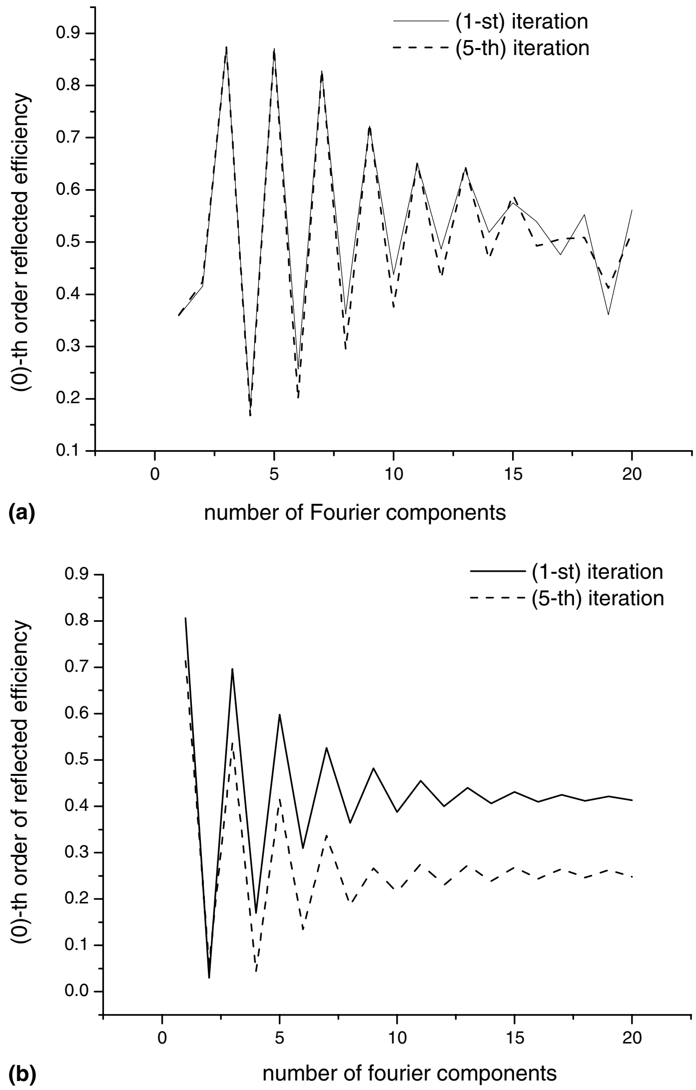

Fig. 5. Convergence of the both classical differential (a) and fast Fourier factorization (b) methods in TM polarization: plot of the reflected efficiency as a function of the number N of Fourier components in linear and nonlinear case. In order to get larger values of the reflected efficiency leading to a better visualization of the convergence, the wavelength is chosen slighty different from the one corresponding to the cavity resonance: $\lambda = 1555$ nm.

vector $\mathbf{F}_{\varepsilon,\omega,\mathrm{NL}}(\mathbf{r})$: there is no Gibbs phenomenon. That is the reason why the reconstruction of the electric field in the coordinate space will be made systematically from the reconstruction of the continuous vector $\mathbf{F}_{\varepsilon,\omega,\mathrm{NL}}(\mathbf{r})$.

3.3. Necessity of the fast Fourier factorization method, in linear and nonlinear optics

The classical differential method uses only the direct rule to calculate the Fourier components of the product in Eq. (14). In Fig. 5(a) is plotted the reflected efficiency as a function of the number of Fourier components using the classical differential method, and as was expected, we can observe the poor convergence of the method. The full line corresponds to the first iteration (linear case) while the dotted line corresponds to the fifth iteration (nonlinear case). As it will be seen in the next section, the fifth iteration is sufficient to take into account the nonlinear effect (Fig. 6). The same plots are then reported in Fig. 5(b) using the FFF method. We see the good improvement of the convergence. Moreover, we can observe that the convergence is slightly slower in the nonlinear case. This phenomenon was expected due to the necessity of the field reconstruction in the nonlinear case.

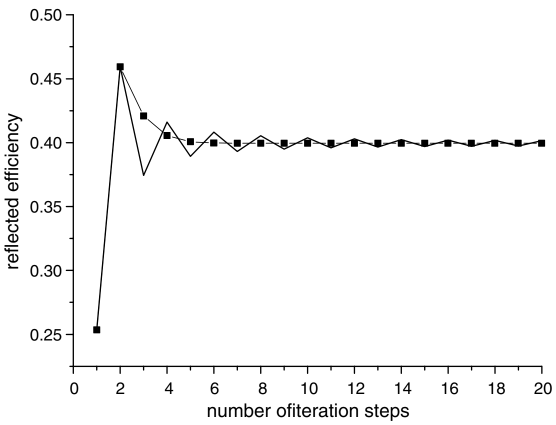

Fig. 6. Representation of the reflected efficiency calculated at different iteration steps. The dielectric permittivity is calculated through Eq. (30) (full line) and Eq. (33) (full line + squares); $\lambda = 1480$ nm, $N = 20$.

3.4. Convergence of the iterative method

Let us now study the convergence of the FFF method as a function of the iteration step number. In Fig. 6 is plotted the zeroth-order reflected efficiency calculated at a wavelength equal to 1500 nm as a function of the number of iteration steps. The nonlinear effect is taken into account from the second iteration and the value of the reflected efficiency converges toward the final result, oscillating around it. From this observation, we can submit a method improving the convergence. The nonlinear dielectric permittivity map calculated at the $\{j-1\}$th iteration step is averaged with the one calculated at the $\{j-2\}$th iteration step

$$\varepsilon_{\omega}^{\{j-1\}}(\mathbf{r}) = \frac{1}{2}\Big(\varepsilon_{\omega,\mathrm{NL}}^{\mathrm{Kerr}\{j-2\}}(\mathbf{r}) + \varepsilon_0\chi_{\omega}^{\mathrm{Kerr}}\mathbf{E}_{\omega,\mathrm{NL}}^{\{j-1\}}(\mathbf{r})\overline{\mathbf{E}}_{\omega}^{\{j-1\}}(\mathbf{r})\Big). \tag{33}$$

The reflected efficiency calculated with the new method (Eq. (33)) is superimposed to the clasical one (Eq. (30)) in Fig. 6; we can observe the nice improvement of the convergence. Indeed, when averaging two successively obtained dielectric permittivity maps, five iterations are sufficient to obtain the convergent result.

3.5. Nonlinear effects in a lamellar metallic grating

The convergence of the method shown in the previous section enables us to study the nonlinear effects on the grating. Using Eq. (33), we plot in Fig. 7 the reflected efficiency as a function of both the number of iterations and the wavelength. The nonlinearity shifts the wavelength of resonance towards larger values. As a consequence, the properties of the grating are modified due to nonlinear effects. This problem is crucial in the design of gratings for high-power lasers. Indeed gratings at these energies may have properties significantly different from those calculated with a linear model. Moreover, our numerical calculations involve a lamellar grating, the differential theory is able to resolve Maxwell equations in many other geometries (sinusoidal, trapezoidal, etc.).

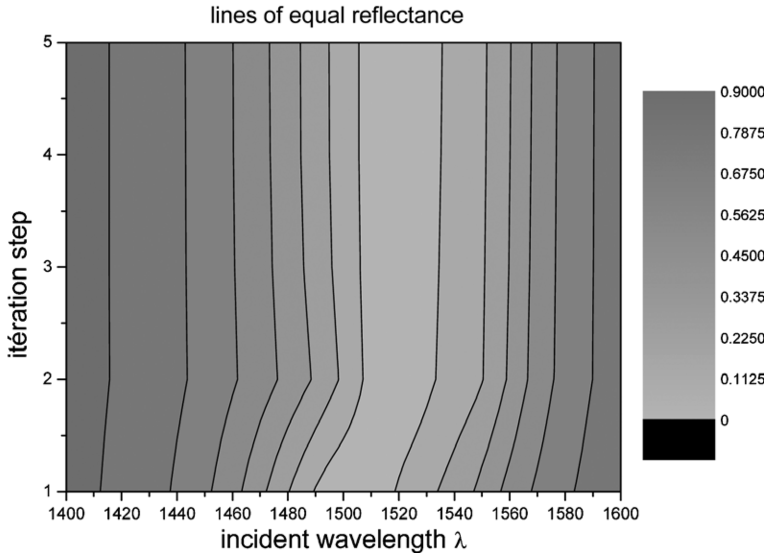

Fig. 7. Representation of the reflected efficiency as a function of both the iteration step amplitude and the wavelength. Visualization of the nonlinear Kerr effect: shift of the wavelength of resonance; $N = 15$. The dielectric permittivity is calculated through Eq. (33).

4. Conclusion

Despite the absence of factorization rule of Maxwell equations in nonlinear periodic media, we have extended the fast Fourier factorization method in nonlinear optics. The iterative method requires the reconstruction of the electric field map inside the grating and the use of the FFT algorithm. The convergence of the method in nonlinear optics with respect to the number of Fourier components is as good as the one obtained with the FFF method in linear optics. The small difference is fully explained by the necessity in the nonlinear case to reconstruct near-field in the nonlinear media, which requires a number of Fourier components larger than the one needed in the calculation of the efficiencies and thus, of the far field. The convergence of the method with respect to the number of iterations with high nonlinear effects is shown, and a method is proposed to increase the convergence speed. It is possible to study strong nonlinear effects in metallic gratings illuminated by plane waves with high amplitude. Devices aimed by this work are gratings used in ultrahigh intensity lasers. Indeed, these lasers use a chirped pulse amplification where a first grating stretches the impulsion, and after amplification of the impulsion energy, a second grating compresses the impulsion. Energies are so high, that Kerr effect in air or in dielectrics may play a non-negligible role in the reflected efficiency value. Such a method is useful to design gratings for high-power lasers.

References

[1] L. Li, J. Opt. Soc. Am. A 13 (1996) 1870.
[2] E. Popov, M. Nevière, J. Opt. Soc. Am. A 18 (2001) 2886.
[3] E. Popov, M. Nevière, N. Bonod, J. Opt. Soc. Am. A 21 (2004) 46.
[4] M. Nevière, E. Popov, Light Propagation in Periodic Media: Differential Theory and Design, Marcel Dekker, New York, 2003.
[5] L. Li, J. Opt. Soc. Am. A 13 (1996) 1024.
[6] R.W. Boyd, Nonlinear Optics, Academic Press, London, 1992.
[7] P. Vincent, N. Paraire, M. Nevière, A. Koster, R. Reinisch, J. Opt. Soc. Am. B 2 (1985) 1106.